UCRL- 91828
PREPRINT

HELIUM-COOLED, FLIBE-BREEDER, BERYLLIUM-MULTIPLIER BLANKET

R. W. Moir
J. D. Lee
R. C. Maninger
W. S. Neef
A. E. Sherwood
D. H. Berwald
J. H. DeVan
J. Jung

This paper was prepared for submittal to
Fusion Technology

March, 1985

Lawrence Livermore National Laboratory

HELIUM-COOLED, FLIBE-BREEDER, BERYLLIUM-MULTIPLIER BLANKET

R. W. Moir*, J. D. Lee, R. C. Maninger, W. S. Neef, and A. E. Sherwood
Lawrence Livermore National Laboratory, University of California
Livermore, CA 94550

D. H. Berwald
TRW
One Space Park
Redondo Beach, CA 90278

J. H. DeVan
Oak Ridge National Laboratory
P.O. Box X
Oak Ridge, TN 37830

J. Jung
Argonne National Laboratory
9700 South Cess Avenue
Argonne, IL 60439

*Mail code: L-644
Telephone: (415) 422-9808

Total number of pages: 54
Total number of tables: 8
Total number of figures: 14

ABSTRACT

The concept described here for the blanket surrounding a fusion reaction chamber is based on the use of molten fluoride salts to convert fusion energy into electricity and to breed the tritium fuel for the fusion power plant. Helium cools the first wall and the blanket internals, which consist of a bed of beryllium balls in which neutrons are multiplied. The neutrons are used to breed tritium and also to release extra energy in exothermic nuclear reactions. Tritium is bred in the molten FLIBE salt (LiF + BeF_2) that flows slowly ($\sim$ 0.1 m/s) in steel tubes, and is removed from the salt and the helium by processing both streams. Because the solubility of tritium in FLIBE salt is so low, there will be a strong driving force for tritium permeation. A 10-μm-thick tungsten permeation barrier, deposited by chemical vapor deposition on the salt-carrying tubes, is proposed for preventing excessive tritium permeation into the helium stream. A 1-mm-thick aluminum jacket on the steel steam generator tubes is proposed to prevent excessive tritium permeation into the steam system. FLIBE salt has safety advantages with respect to large accidents in that it will not react with air or water, in contrast to liquid lithium.

For the first time, a method is proposed for recycling solid material in fusion blankets. To accomplish this, beryllium pebbles were chosen because the pebbles can be loaded into the blanket after manufacturing and, to accommodate radiation induced swelling, can be moved periodically by flowing. Once the balls have reached their radiation-damage lifetime, they can be removed from the blanket for refabrication and recycle.

INTRODUCTION

The helium-cooled, FLIBE-breeder blanket formed the basis for the Princeton Reference Design[1]--the first, large, multidisciplinary study of fusion reactor design study. Tritium breeding was submarginal but this problem was correctable by adding beryllium. A large amount of beryllium in a zone of pebbles 0.4 m to 0.6 m thick resulted in such a good breeder that the idea has formed the basis for fusion-breeder designs.[2,3] One fusion breeder plant of this design can produce 1 GW_e of electricity and enough fissile material (6 tonnes/yr) to fuel fifteen 1-GW_e light-water reactors. The electric power plant version of the fusion reactor was proposed to the Blanket Comparison and Selection Study (BCSS)[4] for evaluation on a common basis with other designs, which are the subjects of companion papers in this issue. The remainder of this paper describes the blanket design and suggests areas for improvement.

MECHANICAL DESIGN

This study developed the blanket design in Fig. 1. Beryllium pebbles, nominally 1 cm in diameter in a 20-cm-thick bed, serve to multiply neutrons. This multiplier zone is concentrically adjacent to a region of silicon carbide (SiC) used to slow neutrons. The neutrons are captured in the lithium-6 within the molten fluoride salt (LiF 47% + BeF 53% with a melting point of 363°C) to breed tritium and release energy in exothermic nuclear reactions. The salt flows slowly through tubes in the blanket and out to a simple flash separator where the tritium is removed. Helium flows radially through the Be pebble bed and SiC region and carries the heat out to the thermal conversion plant. A 10-μm-thick tungsten barrier coats the tubes either on the inside or outside by chemical vapor deposition to cut down tritium permeation to the helium coolant circuit. The tritium inventory for the tungsten barrier on the inside of the tube walls is small and tungsten will contribute to corrosion inhibition. A 1-mm aluminum jacket on the steam generator tubes lowers the tritium permeation to the steam to a predicted value of 55 curies per day. The design can be converted into a fission-suppressed fissile breeder by thickening the beryllium zone by a factor of 2 or so and adding ThF_4 to the salt to produce ∿6 tonnes of uranium-233 per year.

Beryllium is chosen as the neutron multiplier because of it has a large (n, 2n) nuclear reaction cross section and a small cross section for competing side reactions. Compared to other materials, beryllium stands out significantly as a neutron multiplier. This can be seen in the infinite media results of Fig. 2. The material having the next largest neutron multiplication is ^{7}Li.[a] Because its density is lower by a factor of 3.8 than that of beryllium, Li requires a very thick blanket to approach its infinite media multiplication. The multiplication in Pb is much lower than in beryllium but is still quite appreciable.

Some people have thought it inadvisable to use beryllium in fusion-plant designs because it is a limited resource and fusion power would not be inexhaustible. We find beryllium so advantageous that this question needs reexamining carefully. With efficient recycle of used beryllium there is enough beryllium in the U.S. for about 10^4 GW_e years of generation, or roughly the first and second generations of fusion power plants. This would allow fusion to be deployed extensively enough for people to become familiar with the technology. After the first 50-70 years of introduction, the amount of beryllium employed in the blanket might be reduced by more neutronically efficient designs or by achieving better plasma confinement, thus moving towards a D-D fusion fuel cycle that requires lower tritium breeding. Also, with careful design and full recycle of used beryllium resources, fusion power based on the use of beryllium can be considered nearly inexhaustible.

We chose beryllium pebbles to facilitate recycle of irradiated beryllium. A bed of pebbles can, we predict, accommodate some swelling and relative thermal expansion, and can be loaded and unloaded by flowing. We envision factory-made blankets, shipped to the power plant and installed after testing and inspection. The recycled beryllium would have a contact radiation dose rate that would prohibit extensive personnel exposure. Therefore, the pebbles would be loaded into the blanket at the plant. If beryllium or any other recycled material were used in an immobile form, the material would have to be loaded into the blanket during manufacture and, being radioactive, would require remote manufacturing of blankets. No one has shown how to fabricate something as complicated as a blanket by remote methods. Although it can probably be done, the cost may be prohibitive, e.g., greatly exceeding twice the usual manufacturing cost.

FLIBE was chosen as the tritium breeding material. It has a very low corrosion rate with austenitic steel and is predicted to have a low corrosion rate with ferritic steel, provided the salt is kept in a reducing state corresponding to a deficiency of flourine[3]. FLIBE is one of the few lithium-bearing materials that will not react exothermically with air or water. Therefore, accidents due to such reactions will not occur.

The main activation products for both FLIBE and beryllium have relatively short half-lives so that they can be disposed of by shallow burial when necessary. After a ten-year cooling time, some worker radiation protection is needed out of the reactor; however, after 100 years FLIBE and beryllium can be handled without worker radiation protection. FLIBE has an extremely low tritium solubility which leads to very easy tritium removal but also to an increased tendency for tritium to permeate into the helium stream.

The pod design for the helium pressure vessel (see Fig. 1) forms the basis for most of the other helium-cooled designs considered by the BCSS and therefore the first wall, manifolding, plena, and many other shared features do not arise as unique issues when considering the FLIBE design.

Nevertheless, we strongly prefer the ability to gravity drain both the FLIBE and the beryllium pebbles. These objectives were achieved in the design developed for the tandem mirror. However, due to the uniqueness of this among other helium-cooled designs considered in the BCSS, we pursued this design as a backup (see Fig. 3). The end view is shown in Fig. 4. An adaptation to the tokamak configuration has been worked out but is not shown.

The pod modules shown in Fig. 1 are arranged to fit the tokamak configuration as shown in Fig. 5. The module ends, where one sector fits very closely to the next sector is not shown. Much more effort needs to be devoted to module end design because it is not just a design perturbation but has a major impact on blanket design, and is a generic issue.

Tube-Pebble Design Consideration

The salt tubes embedded in the beryllium balls must be spaced so the balls can flow into or out of the tube region without bridging, which would result in flow stoppage. Our flow tests show that if the balls are no larger in diameter than one-half of the free space between tube walls, free flow will occur. Since some balls may crack or swell and develop shape imperfections, we prefer that the ball diameter not exceed one-third of that free space . The pebble size is picked to be large enough to not require excessive pumping power and to permit a reasonable fabrication cost, but small enough to permit free flow between the tubes during pebble changeout and during periodic pebble movement to accommodate pebble swelling. Our nominal values are given in Table I.

The tubes are anchored by clips attaching them to perforated grid spacers not shown in the figures. The tube diameter is sufficiently large that freeze-up will not occur, and sufficiently small so that the centerline temperature will stay well below the boiling point (1300°C at one atmosphere). These limits are discussed in the section dealing with the thermal hydraulic. Nucleonics determines the tube-spacing selection. Too large a spacing will give parasitic loss of neutrons in the beryllium whereas too small a spacing will displace beryllium and reduce fast neutron multiplication. The tube wall thickness should reduce parasitic absorption in the steel and yet be sufficiently thick so as not to buckle when the helium pressure exceeds the salt pressure. Normally, the salt pressure is one atmosphere below the helium pressure, but under abnormal circumstances, the salt may be depressurized to one atmosphere, in which case the tubes will not buckle.

Beryllium and FLIBE Requirements

The salt comprises 9% of the blanket volume, the steel tube walls make up 1% and the steel structure constitutes 5%. In the beryllium zone, the beryllium pebbles take up 53% and the helium occupies 32% of the volume. In the reflector zone, beryllium is replaced by SiC, which comprises 75% of the volume, and the helium occupies 10%. The beryllium zone is 20 cm thick and the SiC zone is 37 cm thick, except on the inside of the tokamak where the SiC zone is only 4 cm thick.

The beryllium zone volume is 0.2 m^3/m^2 of first wall area in a tokamak and 0.23 m^3/m^2 for the tandem mirror. The tandem mirror case is larger due to the small first-wall radius. The volume of the 37-cm-thick SiC region per m^2 is 0.59 m^3 in the mirror and 0.37 m^3 in the tokamak (assuming the same coverage on the inside as the outside). Taking 53% for the volume fraction of beryllium and a full theoretical density of 1.84 g/cm^3 yields 0.20 tonnes/m^2 of beryllium for a tokamak and 0.22 tonnes/m^2 for a mirror. The salt volume is 0.033 m^3/m^2 in a tokamak and 0.053 m^3/m^2 in a mirror. For 3000 MW of fusion power and 5-MW/m^2 wall load, there are 480 m^2 of wall area. The salt volume in the blanket for a tokamak is 16 m^3; in a mirror it is 25 m^3. The mass of beryllium is 96 tonnes in a tokamak and 110 tonnes in a mirror. Finally, there are approximately 100 million 1-cm-diameter pebbles.

Tube-Failure Rate

The breeder-tube-failure rate is a concern because there are so many tubes. For the case of a nominal 4.7-cm-tube spacing on a triangular array, there would be 80,000 tubes in the blanket each having an average length of 11 m. For a rate of one failure per five years, the failure rate per tube per hour of operation must be less than 4×10^{-10}. The helium pressure outside the tube is about 1 atmosphere higher than the pressure of the molten salt in the tube. Small cracks, at welds for example, would result in leakage of helium into the salt but would not constitute a failure. A large crack would result in a large helium-leak rate and would require a shutdown and module change but would have little overall consequence. An offset tube break could contaminate the helium coolant loop with molten salt. This would require a shutdown followed by a cleanup. Analysis should be carried out to determine the tolerable crack size and then to determine if an acceptable failure rate ($< 4\times10^{-10}$ $tube^{-1}$ hr^{-1}) can be achieved.

THERMAL-HYDRAULIC ANALYSIS

As for all fusion blankets, many physics and engineering parameters influence material temperature and heat transfer to the coolant. In performing thermal-hydraulic calculations for the FLIBE/He concept, the first wall flux was assumed to be 5 MW/m^2. The coolant is helium with a nominal pressure of 50 atmospheres. To eliminate pinch-point steam-generator problems, we specified a helium inlet temperature of 275°C. The maximum helium outlet temperature was 500°C in order to keep the structural HT-9 steel below 550°C. We placed this temperature limit on HT-9 steel to avoid the neutron-damage effects that degrade its ductility and strength at higher temperatures.

The blanket energy multiplication ratio has been calculated to be 1.51. Table II shows the calculated energy deposition in the various blanket layers. The blanket analyzed has a first-wall radius of 0.7 m, so each meter of blanket length in a Tandem Mirror Reactor (TMR) produces 33.2 MW of thermal power. The power distribution in the blanket elements is in accordance with the distribution in Table II. Figure 6 was obtained by plotting the three points from Table II that correspond to zones where salt tubes would be present. The first-wall point was ignored because that region is not a breeding zone. The plenum point better defines the energy deposition near the back of the reflector. Power density estimates were made for crucial blanket locations, allowing calculation of the salt tube diameters in those zones.

An assumption that we made not based on detailed calculations was that the helium temperature would increase by 50^{0}C in moving from the plenum chamber to the front wall. This assumption is probably valid for a tokamak where there is considerable first-wall cooling but probably leads to an overestimate of the true value for the tandem mirror. The coolant passes and cools the pod side walls before cooling the first wall, so the blanket-entrance (i.e., approach to the first wall) temperature is to be assumed 325°C.

Table III shows the volumetric heating rates at important blanket locations. These values were obtained by interpolating the plotted data of Table II. To ensure adequate cooling of the salt, we must know the distribution of the neutron-energy deposition among the salt and other blanket elements. Neutronic calculations for the two major zones reveal that in the breeding zone 70% of the energy is deposited in the salt and 30% in the beryllium; in the reflector zone 75% of the energy is deposited in the salt and 25% in the silicon carbide. Table IV summarizes the material fractions in the multiplier and reflector zones. Neglecting heating in the structure, it can easily be shown that the ratios of volumetric energy heat production, q, are

$$q_{salt}/q_{Be} = 13.74 \quad , \tag{1}$$

and

$$q_{salt}/q_{SiC} = 25 \quad . \tag{2}$$

Hence,

$$q_{salt} \times 0.09 + q_{Be} \times 0.53 = 17.6 \times 1.0 \quad , \tag{3}$$

or

$$q_{salt} = 136\ \mathrm{W/cm^3} \quad . \tag{4}$$

Table V summarizes these calculations for the two important blanket zones.

Figures 7 and 8 show the temperature drop across the wall of the salt tube and the film temperature drop at the outside of the salt tube, respectively. Both temperature drops are linear functions of tube diameter if we assume a constant value for the film coefficient. The tube wall temperature depends on the film coefficient at the outside of the tubes. For tubes with polished outsides, the film coefficient h_f will probably range from 0.1 to 0.15 W/cm^2°C. Intentionally roughened tubes with knurl-like exteriors are known to have film coefficients at least a factor of two higher.

Using the factor-of-two enhancement by surface roughening gives a range of h_f (in the tube-size range of interest) from 0.25 to 0.19 W/cm^2°C. This is in good agreement with the bed-of-balls value.[5] We will take a value for h_f of 0.2 W/cm^2°C until experiments can be made involving tubes within packed ball beds.

If we confine the salt to a region having 9% of the multiplier-zone volume, and decide on a staggered tube array (i.e., triangular spacing), one can easily calculate the tube pitch (centerline to centerline) of 2.86 cm and a space between tubes of 1.86 cm. Our tests on ball flow between parallel tubes indicate that the Be ball size should be no larger than 0.33 times the space between tubes. The beryllium balls could therefore be 0.62 cm in diameter, and still be counted on to flow freely into position around the tubes or be readily emptied from the bed when desired. Further design efforts should yield a consistent set of parameters having larger values for these two parameters in order to minimize the number of pebbles and tubes.

It is possible to select smaller tube sizes to reduce the inside-wall temperature of the HT-9 tube. Tube-bank calculations without balls show the increase in h_f as the tube diameter is decreased (see Fig. 9). One pays twice for this higher film coefficient. First the number of tubes in the blanket becomes very large and the tubes are closely spaced. Second, the diameter of the beryllium ball that will still flow through the spaces between tubes becomes very small and an enormous number of balls is required to fill the blanket. Another approach is to increase the volume percentage of breeding salt. Since the same total energy is captured, the tube surface heat flux, hence the wall-film drop, will decrease. Larger tube diameters at the same spacing require smaller beryllium balls. Optimization of the tube diameter, volume fraction of salt, maximum tube-wall temperature, and beryllium-ball diameter must be obtained to yield the lowest cost at an acceptable material temperature.

Table VI shows the coolant temperature as it progresses through the blanket, and the resultant HT-9 temperatures at the inside surface of the salt tubes. The charts of film and wall ΔTs (Figs. 7 and 8) were employed and a tube diameter was chosen for each zone that yielded a temperature slightly below 550°C for the HT-9 salt tubes. Tube sizes vary from 1.0 to 2.0 cm in diameter. It may prove more economical to settle on a single size, e.g., a 1.0-cm-outside diameter, and accept slightly conservative tube temperatures in the other blanket zones.

Thermal-Hydraulic Calculations and Design Improvement

As the coolant moves into the reflector zone, its mean temperature is 442°C. The film temperature drop on the outside of the salt tubes becomes severely limiting. If we could eliminate some of the salt tubes at the rear of the breeding zone and the front of the reflector, the breeding of tritium would be slightly reduced but the temperature limit for HT-9 tubes, 550°C, would not be exceeded in that region of the blanket. This would allow the overall mass flow of coolant to be reduced and would raise the outlet coolant temperature toward the 550°C structure temperature limit, thereby raising the thermodynamic efficiency and reducing the pumping power.

The large number of salt tubes in this design can be reduced by decreasing the fraction of beryllium and increasing the fraction of salt. The smaller neutron multiplication will result in less tritium bred and will also decrease the molten-salt neutron-energy density and allow an increase in tube diameter. The tube spacing must be enlarged as the diameter is increased so that the pebble size can also be enlarged. This results in a smaller number of larger-diameter salt tubes. The tritium breeding ratio in the present design is sufficiently large that a significant reduction can be made.

The reduced fraction of beryllium and increased structure has one more advantage. By capturing more neutrons in structural material, we get a higher energy release than the 4.8 MeV released in the $^6Li(n,T)^4He$ reaction. This larger blanket energy multiplication further assists the economics.

Pressure Drop and Power Loss in Blanket

The velocity of helium coolant based on empty column flow is 144 cm/s. Ergun[6] uses empty column flow to calculate the pressure drop in packed beds such as our beryllium balls surrounded by the steel tubes that carry molten salt. The Reynolds number for this flow is 736. A friction factor, $f_k = 2$, can be read from Fig. 9 of Ergun's paper. The void fraction in this bed of tubes and balls is estimated to be 35%. Using the relationship

$$f_k = \frac{D_p}{L} \frac{\varepsilon^3}{1 - \varepsilon} \frac{\Delta P g_c}{\rho_m U_m^2} \tag{5}$$

where D_p = particle diameter,

ϵ = void fraction of the bed,

ΔP = pressure loss through the bed,

g_c = gravitational constant,

L = length of gas flow (i.e., thickness of the bed)

ρ_m = coolant density

U_m = coolant velocity based on an empty column (i.e., volume flow rate divided by the empty-flow-channel cross-sectional area with no particles present),

one finds the pressure drop to be only 0.07 atmospheres in the 20-cm-deep beryllium-ball multiplier zone, just behind the first wall.

The reflector zone, behind the multiplier zone, is 37-cm deep and is composed of silicon carbide blocks with space (∿2 mm) between each block for helium flow. Because 75% of the reflector is silicon carbide, the gas velocity will be about 600 cm/s. This modest velocity leads to a pressure drop of less than 0.01 atmospheres in this zone. In the back zone where there is more structure and only 53% SiC, the power density is low and cooling becomes easier, especially if we increase the salt volume. When allowance is made for inlet and exit plenum flow losses as well as ball-retention screens, blanket pressure loss will still not exceed 0.1 atmospheres.

If the total thermal power of the reactor is 4000 MW, we calculate that 3432 MW will be developed in the blanket and 568 MW will go to the direct converter. If 225°C is the allowable helium-temperature rise, then 2.94 x 10^6 gm/s of helium must flow through the blanket. This corresponds to 840 m^3/s at a mean density of 0.0035 gm/cm^3. The power consumed in the blanket by the coolant pressure loss is estimated to be 8.4 MW.

NEUTRONICS ANALYSES

Initial scoping calculations were done with the TART[7] code and ENDL[8] data to determine the tritium-breeding potential of this blanket type. In Fig. 10, the tritium breeding ratio (TBR) is shown as a function of Be zone thickness. The value of T is seen to vary between 0.5 for no Be and 1.7 for a 60-cm Be zone. Energy multiplication, M, correspondingly varies between 1.1 and 1.4. The effects of less than 100% blanket coverage on T are also shown for various blanket coverages. For example, if the effective coverage is only 80%, a 15-cm Be zone is needed for T = 1.01, compared to 10 cm at full coverage. A higher T can be achieved of course by increasing the Be zone thickness. The excess neutrons generated in Be might also be used to increase M. While not the objective here, it is clearly possible to include material in the blanket with significantly higher energy release than the 4.8 MeV for the ^{6}Li(n,t) reaction. Also enriching the Li in ^{6}Li can increase the TBR.

The nuclear analysis for the reference tokamak and tandem-mirror-blanket designs has been carried out using the models described in Table VII. The evaluation is based on the MCNP[9] Monte-Carlo[10] method together with the latest version of the ENDF/B-V nuclear data. The statistical mean values are estimated for 10,000 neutron histories in each blanket concept.

The 3-D TBR for the tandem-mirror design is $\sim$1.29 ($\pm$0.9%). Evidently this high TBR has been brought about by the large neutron multiplication of the Be(n,2n) reaction. The reference design, which employs a 20-cm-thick beryllium multiplier (10.6-cm effective thickness), yields a multiplication factor of $\sim$2.0 ($\pm$0.5%). Namely, every neutron born by the D-T fusion is doubled in the FLIBE blanket. This neutron-rich system also yields the substantially high energy multiplication factor of $\sim$1.5 per 14.06 MeV neutron, which is 20 to 40% higher than any other systems investigated in the BCSS study.

The 3-D TBR for the tokamak design is estimated to be ∿1.7 (±0.9%). This can be compared to the full-coverage TBR estimate of ∿1.3 (±0.9%). The most important consideration for the breeding analysis in tokamaks is the presence of any major penetration such as the limiter and rf waveguides. In particular, the selection of limiter design is of great importance in terms of the breeding perturbation to a full breeding blanket. This is not only because a part of the breeding blanket area is lost for the limiter plenum, but because a large number of neutrons are possibly absorbed in the limiter itself. In general, the possible adverse effect on tritium production due to the presence of the limiter would be caused by a drastic spectrum change (softening) in the limiter region, leading to an enhancement of parasitic neutron loss in the limiter materials. In this regard, for the systems where the blanket and limiter designs possess a close spectrum homogeneity (such as the Li/Li and Li/He blankets with the lithium-cooled limiter, and the $LiAlO_2/H_2O$ blanket with the water-cooled limiter), one finds the least adverse effect of the limiter design. On the other hand, the FLIBE design, which employs the water-cooled limiter penetrating through the helium-cooled blanket, suffers from the largest breeding loss.

Table VIII presents a detailed breakdown of the breeding loss for the reference design. It is found that the breeding loss persistently prevails in all three blanket layers (Banks 1 through 3). It is evident from the breakdown by sectors that the breeding is drastically reduced in Sector 7 where the limiter resides and in the closest neighboring sectors (Sectors 6 and 8). The total breeding loss of ∿0.17 is far more than what one can expect from the opening dimensions of the limiter rf penetrations at the first wall, and is rather close to the ratio of the overall limiter-surface area to the total first-wall area, i.e., ∿12% (= 90 m^2/756 m^2).

Based on the 3-D analysis to date, we predict that the reference FLIBE blanket will perform as follows:

	Tokamak	Tandem mirror
TBR	1.17	1.29
E (MeV/ blanket)	20.8	21.0

Based on the initial scoping calculations, we can confidently predict an increase in T and/or M with increasing Be zone thickness.

TRITIUM PERMEATION AND RECOVERY FOR THE FLIBE/He BLANKET DESIGN

A study of tritium permeation and recovery with molten salt for the fusion breeder is reported in Ref. 11. This study assumes tritium to be a gas dissolved in molten salt, with tritium fluoride (TF) formation suppressed.[b] Tritium permeates readily through the hot steel tubes of the reactor and steam generator; it will leak into the steam system at the rate of about one gram per day in the absence of special permeation barriers, assuming that 1% of the helium-coolant flow rate is processed for tritium recovery at 90% efficiency per pass. Tritiated water in the steam system is a personnel hazard at concentration levels well below one part per million and this level would soon be reached without costly isotopic processing. Alternatively, including a combination of permeation barriers on reactor and steam generator tubes, molten salt and helium processing is estimated to reduce the leak rate into the steam system by over two orders of magnitude. For the option with the lowest estimated leak rate, 55 Ci/d, it may be acceptable simply to purge the steam system to prevent tritiated water buildup. At best, isotopic separation of dilute tritiated water may not be necessary and for higher-leak-rate options the isotopic processing rate can be reduced.

The proposed permeation barrier for the reactor tubes is a 10-μm layer of tungsten that, in principle, will reduce tritium blanket permeation by a factor of about 300 below the bare-steel rate. The partial pressure of tritium gas dissolved in molten salt is high, easing the recovery process for which a flash-separator has been chosen. A 1-mm aluminum sleeve is proposed to suppress permeation through the steam generator tubes, giving a calculated reduction factor of more than 500 relative to bare steel, including a factor of 30 due to an assumed oxide layer.

To gain a better understanding of permeation effects, equations describing steady-state tritium permeation without axial flow have been derived for a multilayer tube wall within the blanket region. Although unimportant in our example, a layer of frozen salt is included for generality along with fluid boundary-layer resistances. Calculations of the partial-pressure distribution show significant differences for tubes irradiated at different power densities. Molten-salt boundary-layer resistance can be important in the absence of a good permeation barrier, or for a low-power tube coated with a nominal 1-μm tungsten barrier. Permeabilities of various metals are shown in Fig. 11. The presence of even a thin tungsten barrier will dominate the flow resistance, however, for medium- or high-power-density tubes closer to the first wall. Examination of the radial flux equation reveals a complicated dependence on upstream partial pressure. This dependence reduces to a linear relation at low pressures where Henry's Law materials become flux limiters, and to a square-root dependence at high tritium partial pressures where Sievert's Law materials are flux limiting.

An analytical model has been developed to establish the tritium split between wall permeation and reactor-tube flow. Permeation barriers are shown in Fig. 12. The tungsten coating is shown on the outside of the tubes but could equally well be on the inside. For molten-salt tubes an inside barrier would greatly reduce the tritium inventory in the tube walls and further reduce the already very low corrosion rate. The tritium fraction escaping through the tube walls has been quantified for limiting cases of Henry's Law and Sievert's Law barriers as flux limiters. All parameters of design interest are explicitly included, i.e., tritium generation rates and solubility in salt, tube geometry, barrier permeation parameters, and molten salt processing rate and recovery efficiency.

The intermediate helium heat-transfer loop has been treated as a well-mixed tank for analytical purposes, with tritium input from the molten-salt tubes, with partial tritium recovery in a slipstream process loop, and with Sievert's Law tritium-permeation loss to the steam system.

A combination of effective tritium permeation barriers is required on both blanket and steam generator tubes. Together with substantial process rates for molten-salt and helium systems, the barriers hold tritium permeation into the steam system to 55 Ci/d. If this limit can be met, it may be feasible to simply purge the steam system of incoming tritium, with only minor environmental impact and personnel hazard from steam leaks and without the costly and hazardous isotopic processing to separate tritiated and ordinary water.

A surprisingly thin 10-μm tungsten coating will in principle provide a good permeation barrier on the blanket tubes. The reduction of tritium-blanket permeation by a factor of 300 or so below the bare steel tube rate for some 10^4 m^2 of tube area will require a research and development effort. Although we have focused attention on a tungsten barrier due to a remarkably low tritium permeability, beryllium and other low-permeability materials such as ceramics and cermets should also be considered in barrier development. Other materials or alloys may prove to be superior to tungsten, but probably at the price of greater coating thickness.

A relatively thick 1-mm aluminum sleeve was selected to suppress permeation through the steam-generator tubes. This gave a calculated reduction of more than a factor of 500 relative to bare steel, including a factor of 30 due to an assumed oxide layer. This is essentially a brute force approach that may well be improved upon by the development of more sophisticated permeation barriers.

The tritium-recovery-system flow sheet is shown in Fig. 13. A simple flash separator will allow removal of the tritium and other noncondensable gases, mainly helium, due to the low solubility of tritium in the reducing salt. Tritium removal from helium is virtually a standard process. The bulk of the tritium is recovered as a hydride on a getter bed, with final cleanup accomplished by catalyzed oxidation and adsorption. The diffusivity of tritium gas dissolved in molten salt will need to be measured, especially to verify whether or not the fluid boundary-layer barrier is realistic.

Finally, some definitive experimental work on the kinetics of tritium gas conversion to tritiated water at low concentrations in helium is called for. Popular opinion has vacillated over the last decade between the initial optimism that thermodynamics would reduce the gas concentration to nil, and the current pessimism that predicts no gas conversion at all in the main helium loop. The critical experiments remain to be done with clean walls and particulate-free helium, and in the presence of catalytic surfaces or other reaction promoters. The challenge is to demonstrate a method of drastically reducing tritium gas partial pressure in the intermediate helium loop, thereby suppressing permeation into the steam system.

BERYLLIUM PEBBLE FABRICATION TECHNOLOGIES

Each beryllium pebble is a solid sphere of 1-cm nominal diameter weighing 0.96 g. The pebbles occupy one fuel zone of 20-cm thickness. The calculated mass of beryllium required is 96 tonnes for the tokamak and 110 tonnes for the tandem mirror. Therefore, a nominal mass of 100 tonnes requires about 100 million pebbles for the initial inventory. For an assumed average pebble lifetime of two calendar years, the annual throughput of the hot beryllium fabrication plant will be 5×10^7 pebbles/yr or 50 Tonnes/yr. However, with efficient recycle, the actual beryllium requirement associated with beryllium pebble remanufacture might be 1 to 10%, or 0.5 to 5 MT/yr.

The selected pebble fabrication process involves the development of an automated line that will cold press pebbles, vacuum sinter them, hot forge them to full density, and vacuum anneal them. Brush Wellman currently uses the first three steps of this process to produce aircraft brake segments--the only difference is that the process is manually operated because current Be powder is not free flowing and amenable to automated operations. In order to automate this process, therefore, a free-flowing Be powder is required.

The simple equipment needed for production of spherical beryllium includes mechanical presses and powder feeders to make cold pressed compacts, automated vacuum-sintering furnaces for pressureless sintering, mechanical presses for hot sizing the sintered compacts, and an automated vacuum furnace for annealing the forged compact.

To fabricate pebbles too damaged to reinsert into the blanket after irradiation, we would vacuum melt the hot pebbles and use an automated atomization process (modeled after the Brush Wellman process) to first remanufacture the beryllium powder prior to the cold-press step. We do not exclude the possibility of removing the helium gas by vacuum heating, which would result in about 30% volumetric swelling. These enlarged pebbles might then be pressed back into size. The entire process will require provision for shielding and remote maintainability. In addition, hooding requirements as per OSHA limits ($2 \mu g/m^3$) must be maintained to limit airborne contamination. A beryllium decontamination step (e.g., electro-refining) is not assumed, but might simplify the shielding and remoting requirements.

For a two-year beryllium lifetime,[2,12] assuming an automated plant that operates 24 hours per day, 7 days a week, and that is operating 85% of the time without the production rate must be 110 balls per minute. While this is a very high production rate for Be parts, it is very low for some powder metal industries (e.g., Ta-capacitor manufacturers produce thousands of parts/minute). The beryllium reprocessing line is estimated to lose 7 to 10% of the beryllium throughput, so a small feedstream is required. With a free-flowing powder, the losses might be reduced below 1%.

Preliminary cost estimates for the fabricated beryllium components required to provide beryllium pebbles for the reference tandem-mirror fusion breeder[2] were developed during 1982. These costs were evaluated for the

FLIBE design and an annual cost was estimated. In Fig. 14, a plot of annual beryllium cost vs. pebble size shows the effect on cost of inspection and loss. The cost can be substantially reduced if inspection of each pebble can be eliminated. The loss of beryllium in each manufacturing cycle is unimportant to cost but impacts on resource conservation.

The only special equipment needed for the process line is the air handling system needed to contain the Be powder. The die life should be comparable to those of other powder metallurgy products (500,000 to 1,000,000 parts/die with punches redressed approximately every 500,000 parts). Production of a free flowing Be powder suitable for automated operations requires further development. This might be achieved by a new powder manufacturing technique at Brush Wellman (spherical powder) or by the use of binders which can be totally removed during a bakeout prior to sintering.

Development of a pressing technique which produces a sphere of uniform density that can be pressureless sintered to 90 to 95% of theoretical density is also required. The pressed sphere must be strong enough to permit automated handling. An efficient inspection/test capability may need to be developed if an adequate process reliability cannot be achieved. The technology for carrying out the fabrication process by remote means is expected to be straightforward, but further study is required.

Design Summary and Issues

The key issue with the FLIBE design is tritium control. The tungsten-coated FLIBE tubes and the aluminum jacket, including the oxide layer, on the steam generator tubes must be shown to be workable and reliable as tritium barriers.

Another important issue is the integrity of beryllium during its residence in the blanket. A limited amount of breakup could be tolerated up to the point that flying particles damage the helium circulator or plug the pebble bed. We speculate that a two year residence time (8 MW•y/m^2) would be economically acceptable, after which the pebbles could be remanufactured--especially using the back-up design in which the pebbles could be removed and replaced in less than the blanket-changeout time.

We did not address the question of tritium, which is generated in the beryllium, being released into the helium because this problem was considered unimportant. Only 1% of the total tritium is produced in the beryllium.

Some people believe the remanufacturing of beryllium pebbles will require a large development effort. We believe, however, that use of automated, free-flowing-powder techniques now being implemented in the beryllium industry will allow remanufacturing of these pebbles by straightforward-but-automated powder-metallurgical techniques without a large developmental effort.

Hydrogen (tritium) embrittlement has been flagged as a special problem for the FLIBE design because the tritium concentration estimated for the HT-9 pipes is 1.5 wppm vs. 0.3 to 0.6 wppm for the designs not using FLIBE. This 1.5 wppm was appropriate for the tungsten layer on the outside of the tubes, but on the inside the tritium concentration should go down by a large factor.

The BCSS has flagged corrosion of HT-9 pipes by FLIBE as a significant problem for the FLIBE design. With austenitic steel the corrosion has been shown experimentally to be very small when the salt is maintained in a reducing state, and with ferritic steel we predict it to be very low also. Pumped-loop experiments will be needed to prove the corrosion rates are low, especially in the presence of impurities and for other realistic conditions. MHD and radiation effects are not predicted to be important.

DESIGN IMPROVEMENTS

The pumping power can be reduced by increasing the exit temperature and optimizing the thermal hydraulics (e.g., larger ducts, higher pressure, larger ΔT's). By use of materials which release a larger amount of energy on neutron capture, the energy output can be increased. Both of these improvements should also improve the economics.

CONCLUSION

The FLIBE design appears feasible. If adequate tritium barriers cannot be achieved, the oxidizing state of the salt will be employed to retain tritium as tritium fluoride. A pebble form of beryllium makes use of this element more viable and results in significant and potentially economical advantages not seen in the particular design evaluated in the BCSS. The design, although not scoring highly on safety, appears to cope with accidents by passive means; and because of the low chemical reactivity of the blanket materials, certain kinds of accidents are eliminated. In summary, the FLIBE design should be considered advantageous in the future for the following reasons:

- Relaxed concerns over tritium breeding.
- Enhanced power plant economics from large energy multiplication due to beryllium.
- Inherent safety (no large accidents as there is low chemical reactivity).
- Engineerable design.

This work was performed under the auspices of the U.S. Department of Energy by the Lawrence Livermore National Laboratory under contract number W-7405-ENG-48.

REFERENCES

1. R. G. Mills, Ed., A Fusion Power Plant, Princeton Plasma Physics Laboratory, Princeton, NJ, MATT-1050 (1974).
2. D. H. Berwald, Fission-Suppressed Hybrid Reactor - The Fusion Breeder, Lawrence Livermore National Laboratory, Livermore, CA, UCID-19638 (1982).
3. R. W. Moir et al., Helium-Cooled Molten Salt Fusion Breeder, Lawrence Livermore National Laboratory, Livermore, CA, UCID-20153 (1984).
4. D. L. Smith et al., Blanket Comparison and Selection Study - Final Report, Argonne National Laboratory, Argonne, IL, ANL/FPP-84-1 (1984).
5. S. Whitaker, Fundamental Principles of Heat Transfer, (Pergamon Press, NY, 1977).
6. S. Ergun, "Mass Transfer Rate in Packed Columns," Chemical Engineering Progress 48, (5) (May 1952).
7. R. F. Plechaty and J. R. Kinlinger, TARTNP: A Coupled Neutron-Photo Monte Carlo Transport Code, Lawrence Livermore National Laboratory, Livermore, CA, UCRL-50400, Vol. 14 (1976).
8. R. Howerton et al., The LLL Evaluated Nuclear Data Library (ENDL), Lawrence Livermore National Laboratory, Livermore, CA, UCRL-50400, Vol. 15 (1975).
9. Group X-6, MCNP - Monte Carlo Neutron and Photon Transport, Los Alamos National Laboratory, Los Alamos, NM, LA-7396-M (April 1981).
10. R. Kinsey, Ed., ENDT-102 Data Formats and Procedures for the Evaluated Nuclear Data Files, ENDF, Brookhaven National Laboratory, Upton, NY, BNL-NCS-50496 (ENDF-102) 2nd Ed. (1979).

11. A. E. Sherwood, Tritium Permeation and Recovery for the Helium-Cooled Molten Salt Fusion Breeder, Lawrence Livermore National Laboratory, Livermore, CA, UCID-20141 (1984).

12. L. G. Miller, et al., "Beryllium Lifetime Assessment" in Special Topics Reports For the Reference Tandem Mirror Fusion Breeder, Lawrence Livermore National Laboratory, Livermore, CA, UCID-20166 Vol. 3 (1984).

FOOTNOTES

[a] ^{7}Li is not truly a multiplier but has the same effect due to of the ^{7}Li(n,n'T)^{4}He reaction which produces tritium and preserves the incident neutron.

[b] We have considered the case where tritium is held up as TF in which instance tritium permeation is low but corrosion becomes an issue. The BCSS report (Ref. 4) contains the discussion of this case.

Table I. Nominal pebble/tube parameters.

Tube outside diameter	1.7 cm
Tube spacing	4.7 cm
Tube-wall thickness	0.5 mm
Pebble diameter	1.0 cm

Table II. Blanket energy deposition (ANISN-MACK).

First wall	0.72 MeV
Breeding zone (20 cm)	13.48 MeV
Reflector zone (37 cm)	6.73 MeV
Coolant plenum (22 cm)	0.38 MeV
Total	21.31 MeV per D-T
$M^a = 21.31/14.1 = 1.51$	

[a] Blanket energy multiplication ratio.

Table III. Volumetric heating at key blanket locations.

	Volume (cm^3)	Average volumetric heating (W/cm^3)	Volumetric heating at front of zone (W/cm^3)	Volumetric heating at back of zone (W/cm^3)
Multiplier zone (beryllium balls and salt tubes)	1.19×10^6	17.6	22.1	13.1
Reflector zone (silicon carbide and salt tubes)	2.52×10^6	4.2	7.1	1.4

Table IV. Blanket material fractions.

	Multiplier zone (vol %)	Reflector zone (vol %)
Beryllium	53	--
Silicon carbide	--	75
FLIBE (salt)	9	9
Ferritic steel	6	6

Table V. Energy deposited in salt (W/cm^3).

Multiplier zone		Reflector zone	
Front	Back	Front	Back
172	102	85	17

Table VI. HT-9 tube temperature in the blanket.

Zone	Coolant temperature (°C)	Salt tube diameter (cm)	ΔT °C (film)	ΔT °C (tube wall)[c]	HT-9 temperature at tube I.D. (°C)
Inlet helium	275	--	--	--	--
Entering first wall	325[a]	--	--	--	--
Enter multiplier zone	333[b]	1.1	194	7	534
Exit multiplier zone	442	1.0	103	4	549
Enter reflector zone	442	1.1	96	4	541
Exit reflector zone	496	2.0	39	1	536
Enter helium plenum	500				

[a] Fifty degree temperature rise due to helium cooling of the pod side walls.
[b] Eight degree temperature rise due to helium cooling of the first wall.
[c] Maximum acceptable tube wall temperature = 550°C.

Table VII. System dimensions and zonal material compositions.

Zone	Outer Radius (cm)	Composition
A. Tandem-Mirror Reactor		
Plasma	46	---
Scrape-off	60	---
First wall	66	8.3% HT-9
BANK-1	86	6% HT-9 + 9% FLIBE + 53% beryllium[a]
BANK-2	123	6% HT-9 + 9% FLIBE + 75% SiC
Plenum	145	20% HT-9
Shield	175	Fe-1422 + 20% H_2O
B. Tokamak[b]		
Inboard		
Shield	(415-) 445	80% Fe-1422 + 20% H_2O
Plenum	456	20% HT-9
BANK-2	468	6% HT-9 + 9% FLIBE + 75% SiC
BANK-1	480	6% HT-9 + 9% FLIBE + 53% beryllium[a]
First wall	486	11.7% HT-9
Scrape-off	506	---
Plasma	894	---
Outboard		
Scrape-off	914	---
First wall	920	11.7% HT-9
BANK-1	940	6% HT-9 + 9% FLIBE + 53% beryllium[a]
BANK-2	952	6% HT-9 + 9% FLIBE + 75% Sic
BANK-3	977	28% HT-9 + 9% FLIBE + 53% SiC
Plenum	999	20% HT-9
Shield	1029	80% Fe-422 + 20% H_2O

[a]Beryllium: 100% theoretical density.

[b]Based on a major radius model at the reactor midplane.

Table VIII. The impact of limiter/rf design on tritium breeding[a] for the Tokamak/FLIBE/He-HT9-Be design.

Region	3D-TBR Full breeding		3D-TBR with limiter rf		Relative difference (%)	Net breeding loss
Bank-1	0.993	(±1.0%)	0.866	(±1.1%)	-12.8	-0.127
Bank-2	0.140	(±2.0%)	0.124	(±2.1%)	-11.1	-0.016
Bank-3	0.208	(±1.9%)	0.184	(±2.0%)	-11.7	-0.024
Sector-1	0.189	(±2.4)	0.171	(±2.5%)	- 9.1	-0.017
Sector-2	0.064	(±4.4)	0.063	(±4.4%)	- 0.9	-0.001
Sector-3	0.093	(±3.6)	0.086	(±3.9%)	- 7.6	-0.007
Sector-4	0.294	(±2.1)	0.271	(±2.1%)	- 7.8	-0.023
Sector-5	0.259	(±2.2)	0.262	(±2.2%)	0.9	0.002
Sector-6	0.290	(±2.1)	0.250	(±2.2%)	-13.7	-0.040
Sector-7	0.088	(±3.7)	0.025	(±5.9%)	-71.3	-0.062
Sector-8	0.065	(±4.2)	0.045	(±5.4%)	-30.4	-0.020
Total						
T_6	1.330	(±0.9%)	1.164	(±0.9%)	-12.5	-0.166
T_7	0.011	(±0.9%)	0.010	(±1.0%)	- 9.9	-0.001
$T_6 + T_7$	1.341	(±0.9%)	1.174	(±0.9%)	-12.5	-0.167

[a]Based on MCNP/ENDF/B-V evaluation with 10,000 neutron histories.

FIGURE CAPTIONS

Fig. 1. Helium-cooled, FLIBE blanket with beryllium as the neutron multiplier.

Fig. 2. Neutron multiplication for various materials. Beryllium has the highest multiplication for nonfissioning materials.

Fig. 3. He/FLIBE/Be--tandem mirror backup design.

Fig. 4. End view of molten salt blanket. The figure shows the cross section looking down the axis of the central cell.

Fig. 5. Tokamak module and piping arrangements.

Fig. 6. Neutron energy deposition in molten-salt breeding blanket.

Fig. 7. Temperature drop through wall of molten salt tube. The wall thickness is 0.5 mm. The HT-9 steel has a thermal conductivity of 0.29 W/cm°C. Cases are differentiated by the amount of volumetric energy deposited in the salt.

Fig. 8. Temperature drop through outside coolant film on the salt tube. The helium film coefficient is 0.2 $W/cm^2 °C$. The wall thickness is assumed to be 0.5 mm. Cases are differentiated by the amount of volumetric energy deposited in the salt.

Fig. 9. Surface film coefficient of heat transfer at outside of tube vs tube diameter. The film coefficient assumes helium present at 50 atm, cross flow, and a tube surface roughened to double the smooth-tube h_f.

Fig. 10. Tritium-breeding ratio for FLIBE blanket vs. Be zone thickness.

Fig. 11. Permeation coefficient of tritium through metals.

Fig. 12. Permeation geometry and materials.

Fig. 13. Molten-salt tritium processing flow sheet.

Fig. 14. Annual beryllium cost versus pebble size showing the effect on cost of inspection and loss. The reference case is for 5×10^7 pebbles/yr and includes both materials and fabrication.

R. W. Moir et al. - Fig. 1

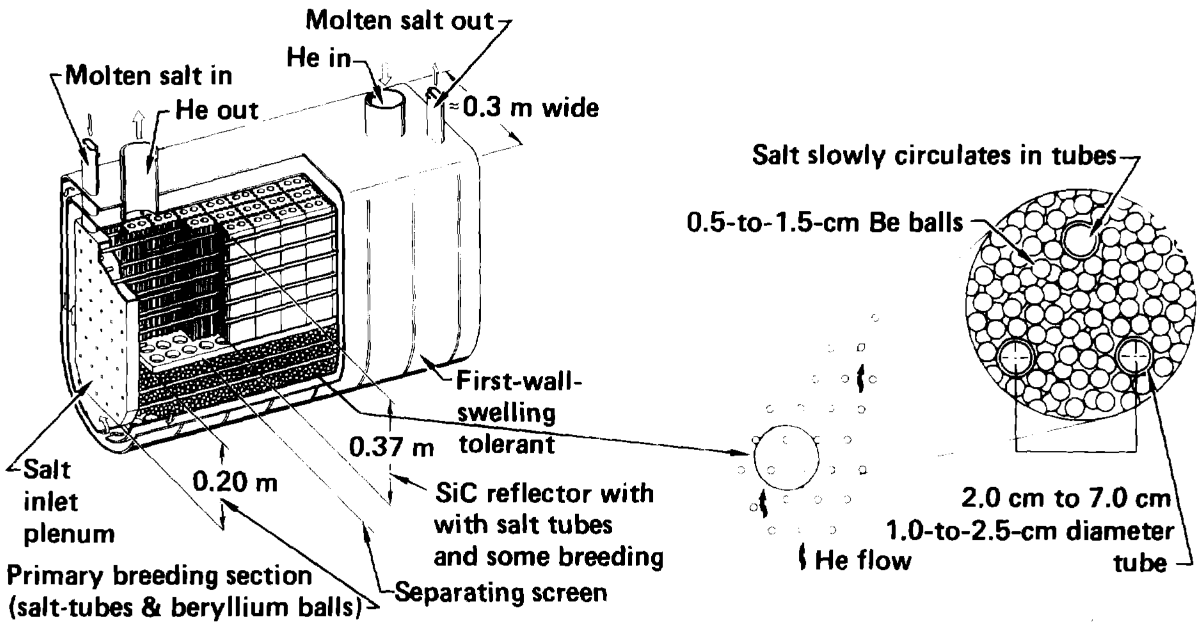

R. W. Moir et al. - Fig. 2

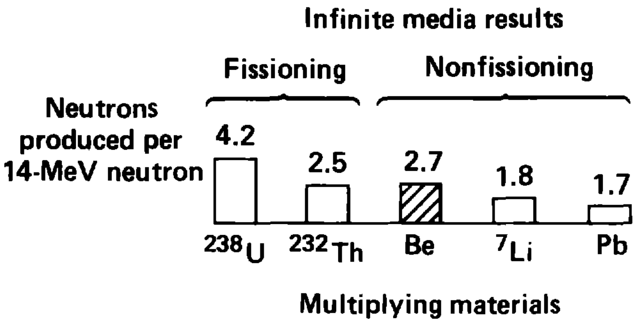

R. W. Moir et al. - Fig. 3

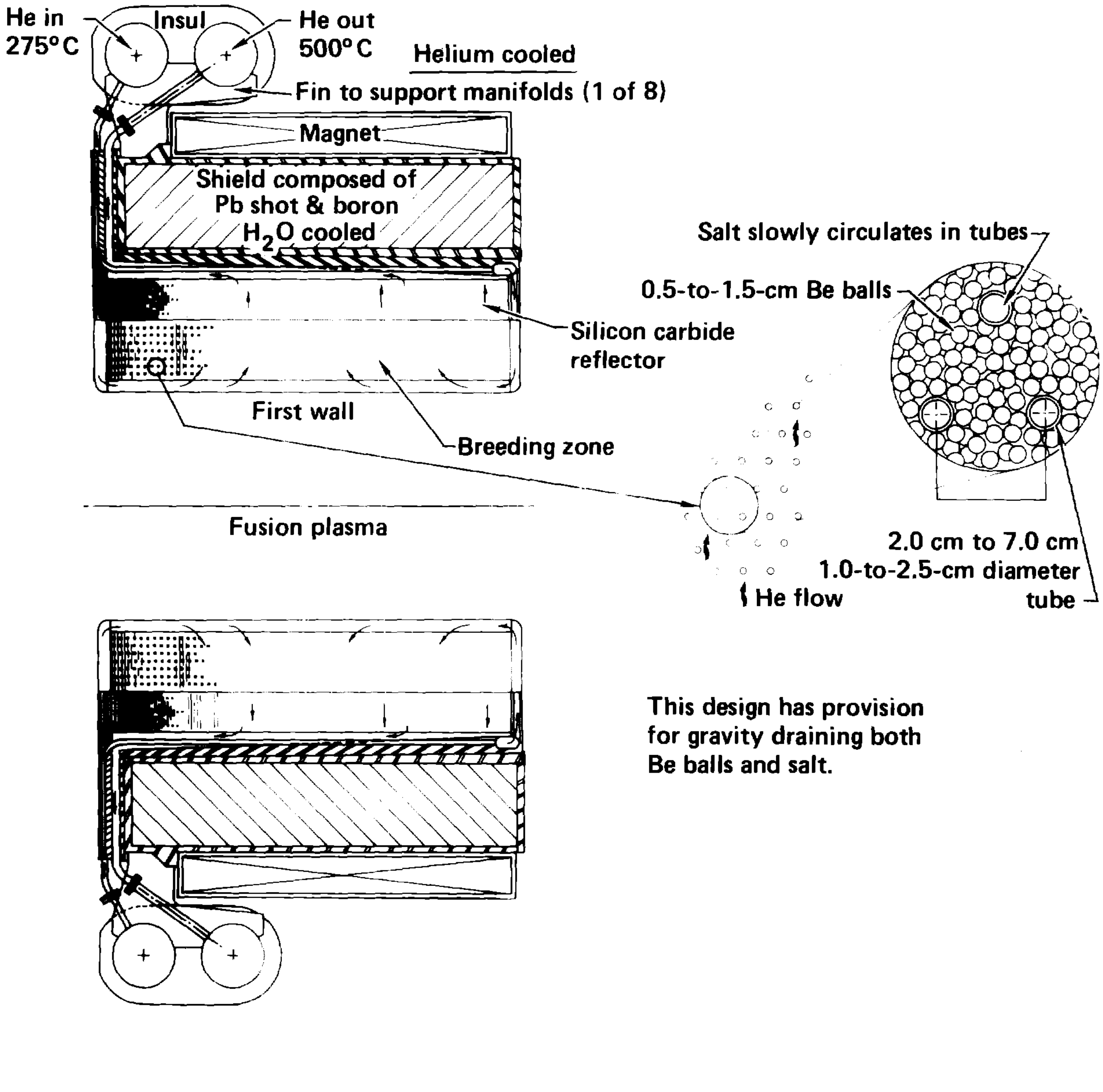

This design has provision for gravity draining both Be balls and salt.

R. W. Moir et al. - Fig. 4

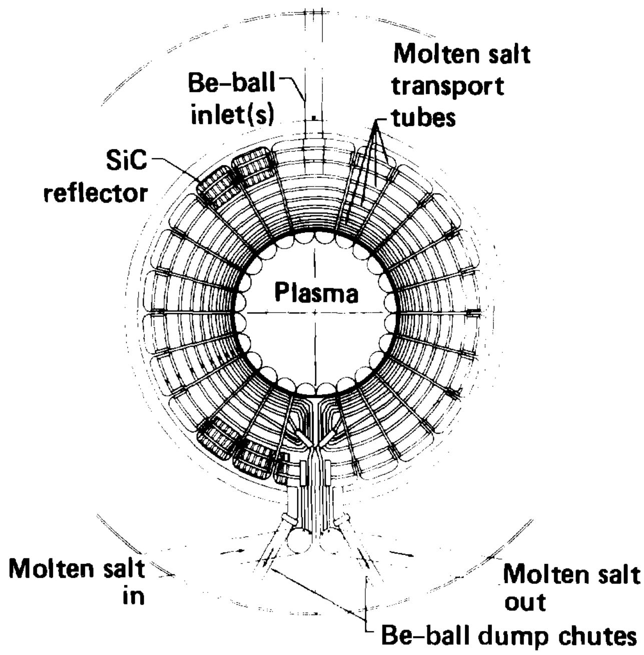

Space between tubes filled with beryllium balls

R. W. Moir et al. - Fig. 5

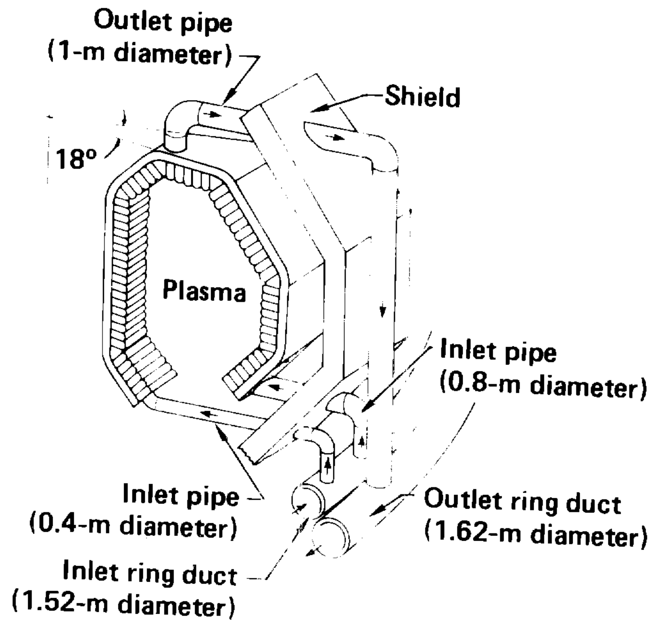

R. W. Moir et al. - Fig. 6

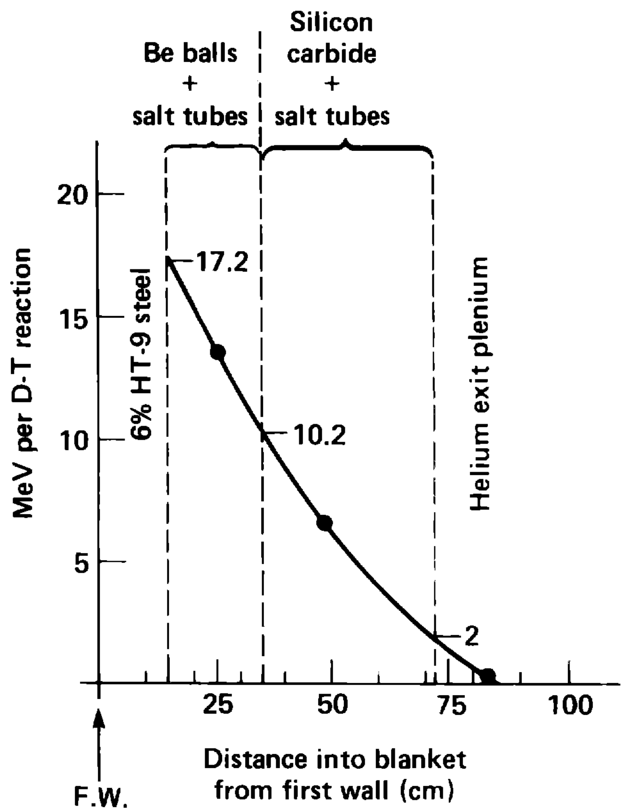

R. W. Moir et al. - Fig. 7

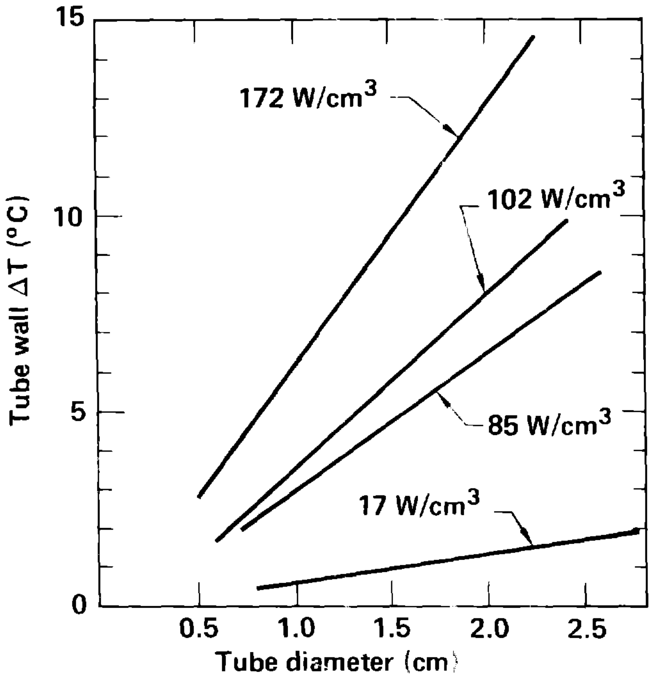

R. W. Moir et al. - Fig. 8

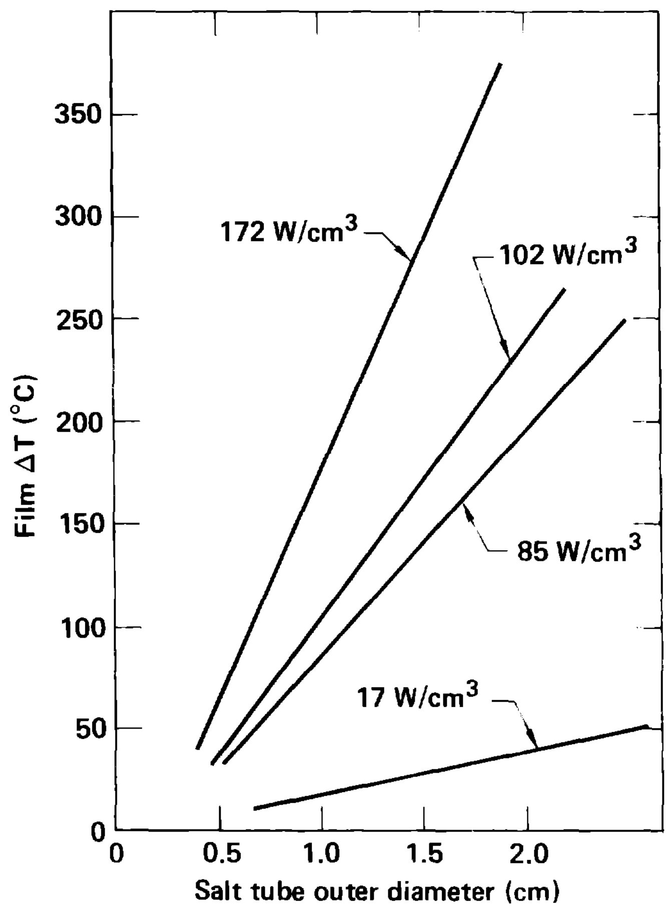

R. W. Moir et al. - Fig. 9

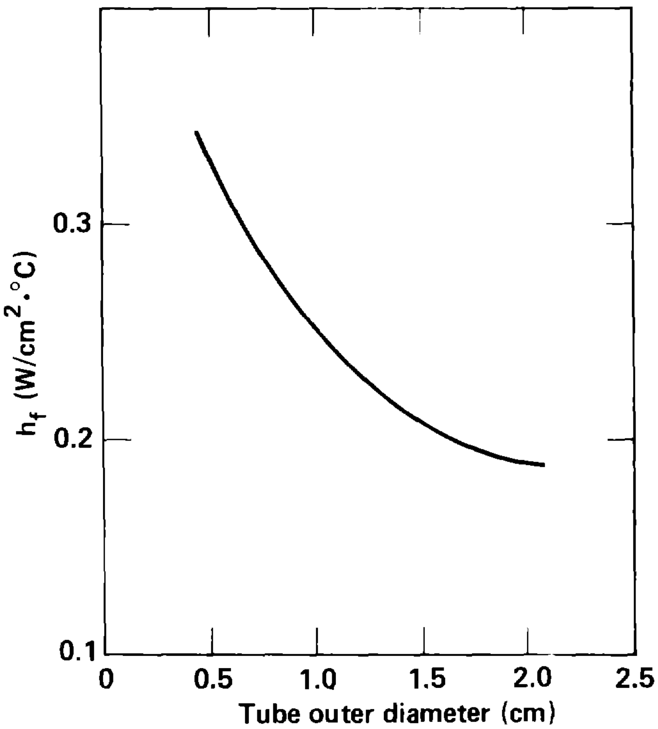

R. W. Moir et al. - Fig. 10

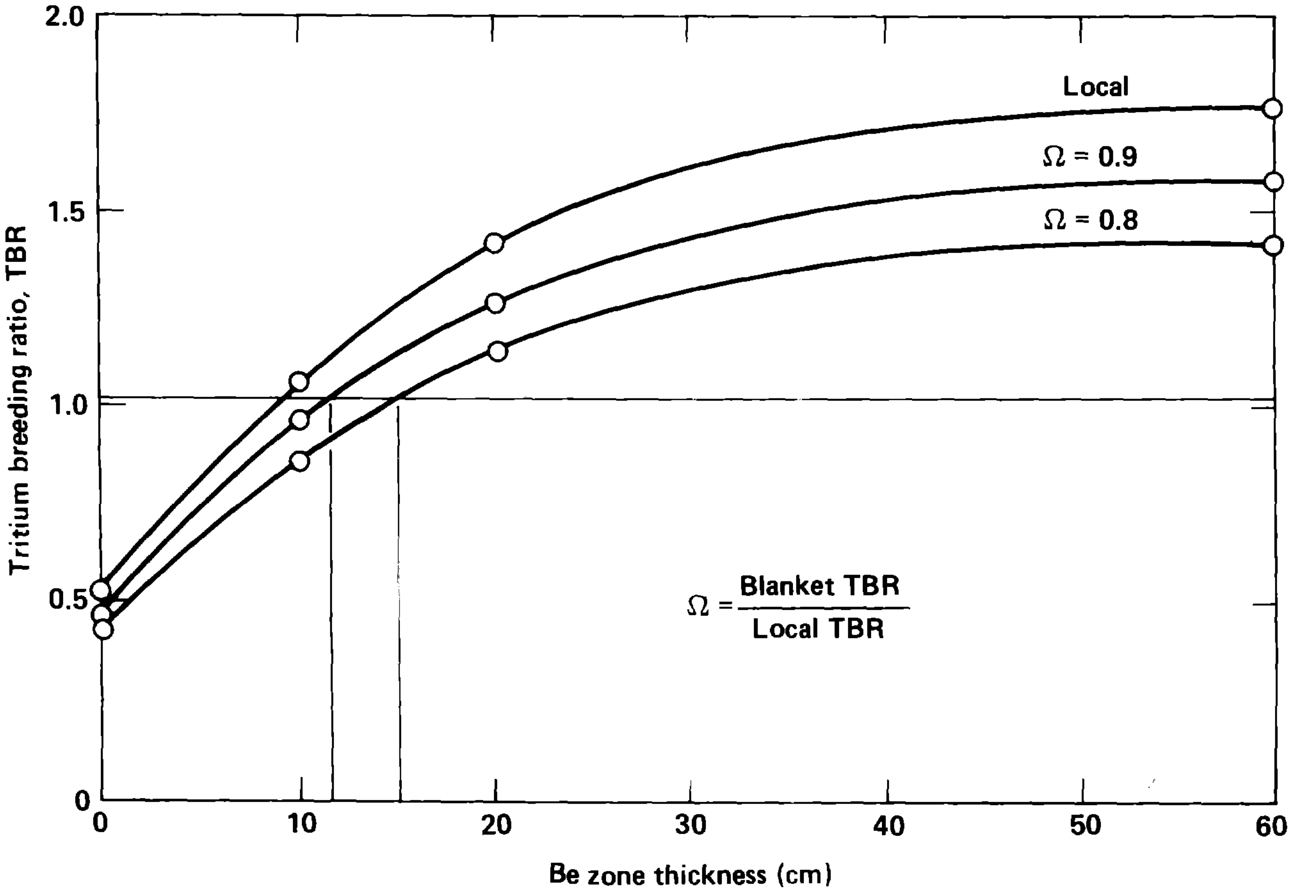

R. W. Moir et al. - Fig. 11

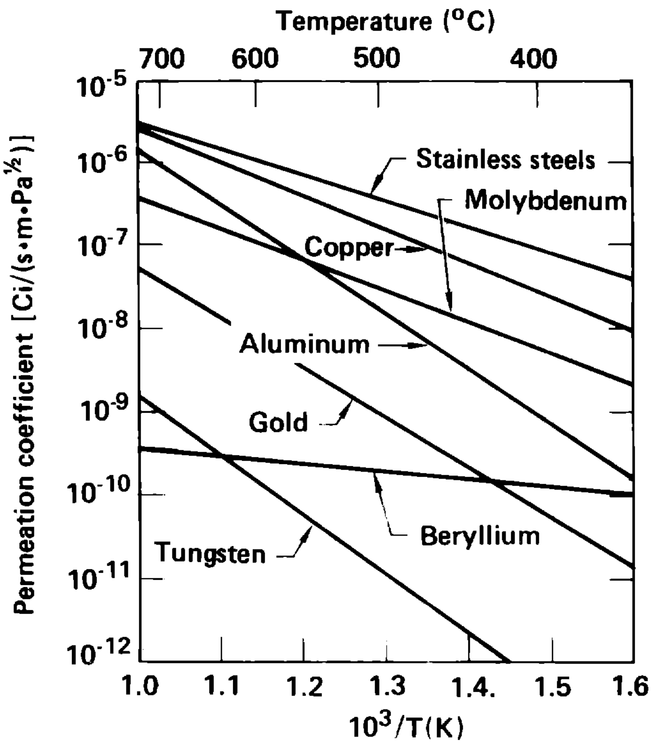

R. W. Moir et al. - Fig. 12

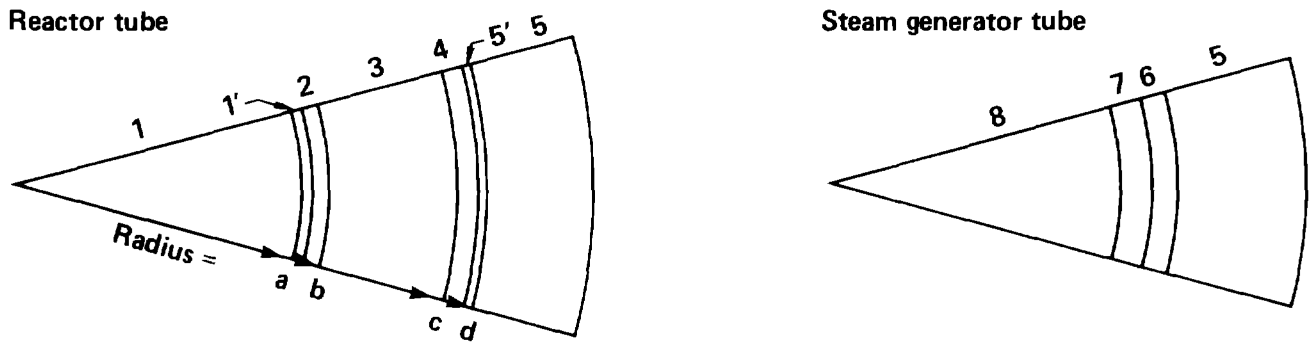

1 Molten salt
1' Molten salt boundary layer
2 Frozen salt
3 Stainless steel tube
4 Permeation barrier (tungsten)
5' Helium gas boundary layer
5 Helium gas

5 Helium gas
6 Permeation barrier (aluminum)
7 Stainless steel tube
8 Water/steam

R. W. Moir et al. - Fig. 13

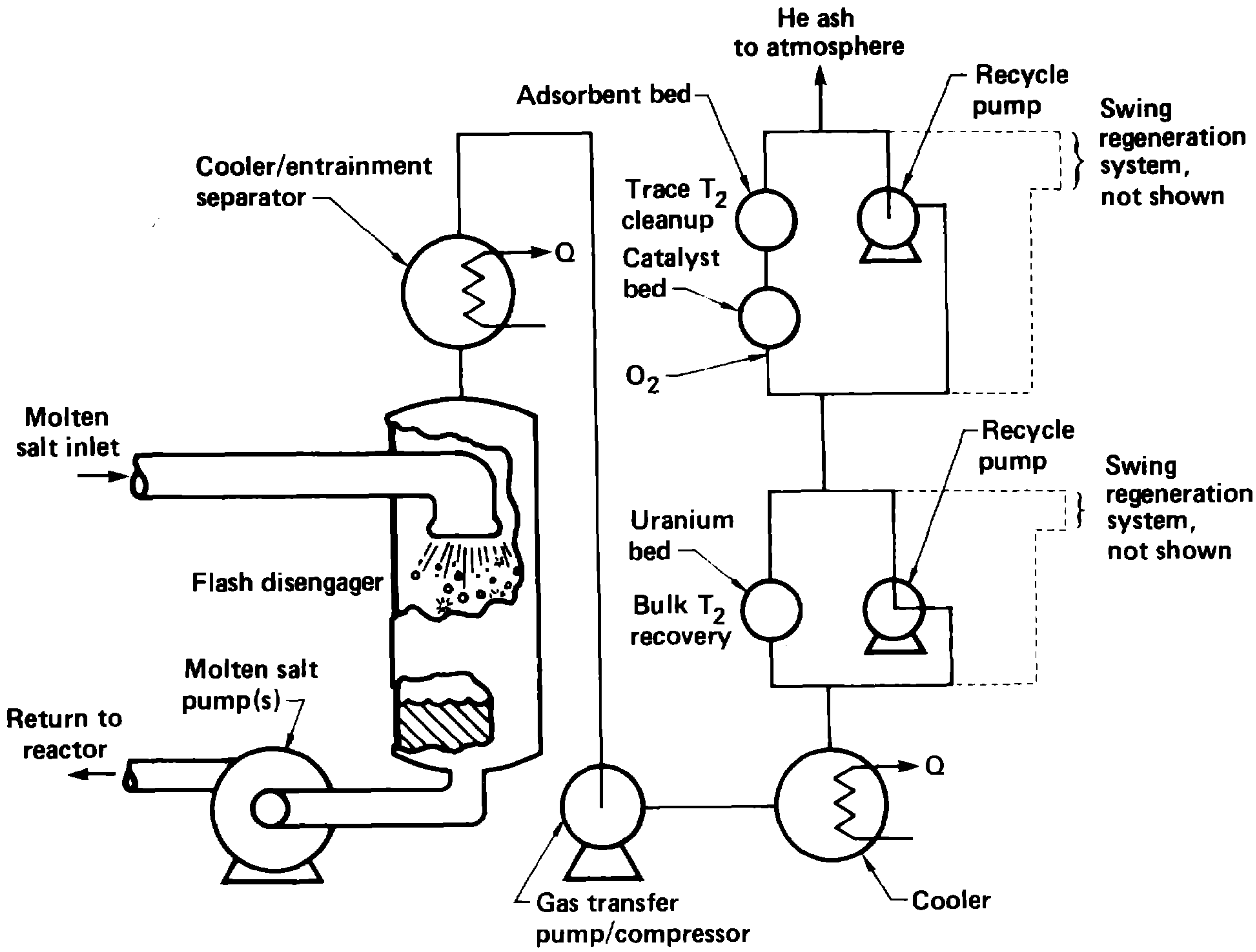

R. W. Moir et al. - Fig. 14